Accuracy of Single-Voxel Proton MR Spectroscopy in Distinguishing Neoplastic from Nonneoplastic Brain Lesions

S. D. Rand, R. Prost, V. Haughton, L. Mark, J. Strainer, J. Johansen, T. A. Kim, V. K. Chetty, W. Mueller, G. Meyer, and H. Krouwer

PURPOSE: To measure the accuracy of single-voxel, image-guided proton MR spectroscopy in distinguishing normal from abnormal brain tissue and neoplastic from nonneoplastic brain disease. **METHODS:** MR spectroscopy was performed at 0.5 T with the point-resolved spectroscopic pulse sequence and conventional postprocessing techniques. Subjects consisted of a consecutive series of patients with suspected brain neoplasms or recurrent neoplasia and 10 healthy adult volunteers. Fifty-five lesions in 53 patients with subsequently verified final diagnoses were included. Spectra were interpreted qualitatively by visual inspection by nonblinded readers (prospectively) with the benefit of prior clinical data and imaging studies, and by blinded readers (retrospectively). The nonblinded readers interpreted the spectra as diagnostic or not, and, if diagnostic, as neoplastic or nonneoplastic. The blinded readers classified the spectra as diagnostic or not, and, if diagnostic, as normal or abnormal and as neoplastic or nonneoplastic (when abnormal). The sensitivity, specificity, positive and negative predictive values, and accuracy were calculated from blinded and nonblinded MR spectroscopy interpretations. A receiver operator characteristic (ROC) curve analysis was performed on blinded MR spectroscopy interpretations. **RESULTS:** The diagnostic accuracy averaged across four blinded readers in differentiating patients from control subjects was .96, while the area under the aggregate (pooled interpretations) ROC curve approached unity. Accuracy in the nonblinded and blinded discrimination of neoplastic from nonneoplastic disease was .96 and .83, respectively. The area under the aggregate ROC curve in the blinded discrimination of neoplasm from nonneoplasm was .89. **CONCLUSIONS:** Image-guided proton spectra obtained at 0.5 T from patients with suspected neoplasia can be distinguished from spectra in healthy control subjects, and neoplastic spectra can be distinguished from nonneoplastic spectra with a high degree of diagnostic accuracy.

Index terms: Brain neoplasms, magnetic resonance; Magnetic resonance, spectroscopy

Magnetic resonance (MR) spectroscopy at 1.5 to 4.0 T (1–7) and at 0.5 T (R. W. Prost, W. Mueller, Z. Yetkin, L. Hendrix, V. Haughton, "0.5 T H-1 Spectroscopy as an Adjunct to Diagnosis in Indeterminate CNS Lesions: Results for 40 Patients," presented at the annual meeting of the Society of Magnetic Resonance in Medicine, Nice, France, August 1995) consistently demonstrates an elevation of choline (Cho) levels and a depression of N-acetylaspartate (NAA) resonances in nonnecrotic portions of brain neoplasms (8–10). These studies suggest that MR spectroscopy might be useful in differentiating neoplasms from nonneoplastic lesions that simulate neoplasms on imaging studies. We measured the diagnostic accuracy of MR spectroscopy at 0.5 T in distinguishing normal from abnormal spectra and neoplastic from nonneoplastic brain disease using binary decision statistics and receiver operator characteristic (ROC) curve analysis.

TABLE 1: Binary decision matrix summary

	Normal versus Abnormal Spectra						Tumor versus Nontumor					
	No.	Sensitivity	Specificity	Positive Predictive Value	Negative Predictive Value	Accuracy	No.	Sensitivity	Specificity	Positive Predictive Value	Negative Predictive Value	Accuracy
Nonblinded readers							54	.95	1.00	1.00	.86	.96
Reader A	56	0.96	0.90	0.98	0.82	.95	46	.78	1.00	1.00	.53	.83
Reader B	58	1.00	0.80	0.96	1.00	.96	48	.97	0.67	0.90	.89	.90
Reader C	61	0.96	1.00	1.00	0.83	.97	51	.82	0.67	0.89	.53	.78
Reader D	58	0.96	1.00	1.00	0.83	.96	48	.84	0.60	0.89	.50	.79
Average*	58	0.97	0.93	0.99	0.87	.96	48	.85	0.74	0.92	.61	.83

Note.—No. signifies the number of cases evaluated by each reader.
*Arithmetic mean values from individual readers.

Materials and Methods

Patients with suspected neoplastic brain lesions on computed tomographic (CT) or MR imaging studies were examined with MR spectroscopy. All patients studied between September 1994 and December 1995 in whom diagnoses were verified by histologic examination or by appropriate laboratory studies or clinical follow-up were included. MR spectroscopy was also performed in the cerebrum of 10 healthy adult control subjects.

Spectra from patients were acquired on a clinical 0.5-T system with a prototype quadrature receive/transmit head coil or a receive-only conformal surface coil (11) (Prost et al, "0.5 T H-1 Spectroscopy..."). The point-resolved spectroscopic (PRESS) pulse sequence was used with chemical-shift selective (CHESS) water suppression (1500/41/256 [repetition time/echo time/excitations]) and conventional postprocessing techniques (11). Additional spectra with echo times of 272 were obtained in those cases in which mobile lipid resonances obscured metabolites in the range of 0.5 to 1.5 ppm. Cubic or nearly cubic MR spectroscopic voxels were centered over solid portions of the lesions to sample the most metabolically active tissue and to avoid necrotic debris or edema whenever possible. A compromise between partial volume effects with large voxels and poor signal-to-noise ratio (SNR) with small voxels determined a typical voxel size of 1 to 3 cm^3. (MR spectroscopy was discouraged for lesions less than approximately 1 cm^3.) Regions that had shown contrast enhancement on prior studies were sampled whenever possible. Localizer images and spectra were typically acquired within 45 minutes. Resonance assignments were as follows: mobile lipids (Lip), 0.5 to 1.5 ppm; lactate doublet (Lac), 1.15 and 1.50 ppm; creatine (Cr), 3.04 ppm; NAA, 2.02 ppm; the combination (Glx) of glutamine and glutamate, 2.35 to 2.46 ppm; Cho, 3.21 ppm; and *myo*-inositol (m-Ins), 3.54 to 3.63 ppm.

Before the acquisition of prototype receiver coils, control spectra were obtained with a standard head coil, with which voxels of 8 cm^3 provided satisfactory SNR. All other hardware, pulse sequence parameters, and postprocessing techniques were identical to those of the patient examinations. For each control subject, a mixture of cortex and subcortical white matter at the same location within the posterior left frontal lobe was sampled at the level of the lateral ventricles, as determined by axial T2-weighted localizer images.

Spectra were interpreted by visual inspection, analogous to the qualitative interpretation of other graphical data, such as electrocardiographic or electroencephalographic recordings. At the time of MR spectroscopy, one of four nonblinded neuroradiologists and an MR spectroscopist generated a formal written (prospective) report with the benefit of prior clinical data and imaging studies. The nonblinded readers interpreted the spectra as diagnostic or not, and, if diagnostic, as neoplastic or nonneoplastic. Subsequently, spectra were interpreted retrospectively by four blinded neuroradiologists. The blinded readers classified the spectra as diagnostic or not, and, if diagnostic, as normal or abnormal and as neoplastic or nonneoplastic (when abnormal). Individual blinded and nonblinded readers were given the discretion to declare a spectrum as nondiagnostic if the technical quality was insufficient or if the findings were equivocal, with the understanding that nondiagnostic examinations could be repeated at the same location or at a different site (as needed), as per our current clinical practice. (By necessity, patients were typically discharged from the MR suite before spectra could be postprocessed off-line, checked for technical quality, and interpreted.) This resulted in different sample sizes (No.) for the blinded readers in Tables 1 through 4.

Nonblinded (prospective) readers included four attending physicians with between 6 and 20 years of neuroradiologic experience, and up to 1 year of clinical experience with MR spectroscopy. Blinded (retrospective) readers included a staff neuroradiologist with 20 years' experience, 1 year of which included MR spectroscopy (reader A); a staff neuroradiologist with 6 months' experience, 4 months of which included MR spectroscopy (reader B); a visiting staff neuroradiologist with 12 years' experience, 2 weeks of which included MR spectroscopy (reader C); and a first-year neuroradiology fellow with 2 months' experience with MR spectroscopy (reader D). One of the neuroradiologists (reader A) participated in both blinded and nonblinded interpretations.

TABLE 2: ROC curve summary

	Normal versus Abnormal Spectra					Tumor versus Nontumor				
	No.	Az	(SD)	Aw	(SD)	No.	Az	(SD)	Aw	(SD)
Reader A	56	.98	(.020)	.98	(.015)	46	.94	(.037)	.94	(.033)
Reader B	58	DD	⋯	DD	⋯	48	NCD	NCD	.91*	⋯
Reader C	61	DD	⋯	DD	⋯	51	.84	.065	.84	(.058)
Reader D	58	DD	⋯	DD	⋯	48	.90	.048	.88	(.051)
Aggregate	233	.99	(.007)	.99	(.006)	193	.84	.020	.89	(.024)
Average	⋯	⋯	⋯	⋯	⋯	48	.89	⋯	.89	⋯

Note.—No. signifies the number of cases evaluated by each reader; Az, the area under the (continuous) estimated ROC curve; Aw, the trapezoidal area under the (discrete) ROC curve. ROC operating points and estimated ROC curve were obtained from aggregate (pooled) data; average signifies the arithmetic mean values from individual (nonpooled) estimated ROC curves (where available); DD signifies that data were (mathematically) degenerate and implied near-perfect decision performance; NCD signifies that the algorithm to estimate a continuous ROC curve did not converge within 100 iterations.

* Aw calculated graphically from the discrete ROC operating points.

TABLE 3: κ statistics summary

	κ Normal versus Abnormal					κ Tumor versus Nontumor				
	No.	Reader A	Reader B	Reader C	Reader D	No.	Reader A	Reader B	Reader C	Reader D
Reader A	56	⋯	.81	.94	.84	46	⋯	.54	.55	.64
Reader B	58	⋯	⋯	.76	.76	48	⋯	⋯	.57	.54
Reader C	61	⋯	⋯	⋯	.89	51	⋯	⋯	⋯	.51
Reader D	58	⋯	⋯	⋯	⋯	48	⋯	⋯	⋯	⋯

Note.—No. signifies the number of cases evaluated by each reader; κ, strength of agreement: <.20, poor; .21–.40, fair; .41–.60, moderate; .61–.80, good; and .81–.94, very good.

For blinded (retrospective) interpretations, control and patient spectra were presented in random order. Blinded readers were required to assign metabolites to resonance peaks without assistance from the MR spectroscopist. Readers were provided with an example of a control spectrum at echo times of 41 and 272, a list of resonance assignments adapted from the literature, and an assortment of recent articles on MR spectroscopy for reference. Because the blinded interpretations were made retrospectively, and because some cases had been discussed previously in radiologic or neuroscientific conferences at our institution, blinded readers were asked whether they recognized any spectra as belonging to a particular patient. If so, the case was excluded from the analysis. The binary decision statistics (sensitivity, specificity, and so forth) were calculated for the whole study sample and then separately for the untreated and previously treated patients. Control spectra were excluded from the analysis of neoplasm versus nonneoplasm so as to avoid biasing the results toward a higher specificity.

The MR spectroscopic interpretations were based primarily on the amplitudes of the NAA, Cho, and Glx resonances relative to Cr. Specific criteria for MR spectroscopic differential diagnosis, based on observations at our institution and in the literature, are summarized in Table 5. An ordinal 9-point scale (12) was chosen for convenience, analogous to ordinal scales used in physical diagnosis for motor strength, reflexes, and so on. The diagnostic sensitivity, specificity, positive predictive value (PPV), negative predictive value (NPV), and accuracy of blinded and nonblinded interpretations were computed with standard formulas (13, 14).

Spectra were scaled by the blinded readers from 1 to 100 as normal or abnormal, and as neoplastic or nonneoplastic. A higher score in response to normal or abnormal represented a higher probability of an abnormal spectrum. Similarly, a higher score in response to neoplastic or nonneoplastic represented a higher probability of a neoplastic spectrum. For the purpose of a κ analysis of interobserver variability (described below), and for binary decision statistics (sensitivity, specificity, and so on), the blinded readers' scores from 1 to 50 and from 51 to 100 were defined as negative and positive, respectively.

The full range of 1 to 100 was used to construct ROC curves for each reader and for the aggregate (pooled interpretations) (14, 15) with a computer program (labroc1, C. E. Metz, University of Chicago [Ill]). Maximum likelihood estimates of continuous binormal ROC curves and continuous (Az) and trapezoidal (Aw) areas under the curves were calculated. If the estimation algorithm did not converge to provide a continuous curve after 100 iterations, only the discrete ROC operating points were used to calculate the trapezoidal (Aw) area.

Interobserver variability of the blinded MR spectroscopy interpretations was measured with nonweighted κ statistics (Stata, Stata Corp, Santa Monica, Calif). A paired analysis of variance (ANOVA) (Instat, Graphpad Software, San Diego, Calif) was used to test the null hypothesis that there

TABLE 4: Binary decision matrix summary

| | Untreated Patients | | | | | | Treated Patients | | | | | |
| | Tumor versus Nontumor | | | | | | Tumor versus Nontumor | | | | | |
	No.	Sensitivity	Specificity	Positive Predictive Value	Negative Predictive Value	Accuracy	No.	Sensitivity	Specificity	Positive Predictive Value	Negative Predictive Value	Accuracy
Reader A	33	0.80	1.00	1.00	0.62	.85	13	.75	1.00	1.00	.25	.77
Reader B	35	1.00	0.73	0.90	1.00	.91	13	.92	0.00	0.92	.00	.85
Reader C	37	0.81	0.80	0.92	0.62	.81	14	.83	0.00	0.83	.00	.71
Reader D	35	0.92	0.67	0.90	0.75	.86	13	.67	0.00	0.90	.00	.62
Average	35	0.88	0.80	0.93	0.75	.86	13	.79	0.25	0.91	.06	.74

Note.—No. signifies the number of cases evaluated by each reader; average signifies the arithmetic mean values from individual readers.

TABLE 5: Differential diagnosis of brain proton MR spectroscopy

Diagnosis	Cho	Cr	Glx	NAA	Lipid	Lactate
Glioblastoma	−− to ++	−−	−−	−−−	+++ to ++++	+++ to ++++
Glioma (other)	++ to +++	− to −−	−−	− to −−−	Absent to +	Absent to ++
Lymphoma	++++	−−	− to −−	−−−	Absent to ++	Absent to ++
Meningioma	++++	−−−	Normal to −−	Absent to −−−	+ to ++	Absent to +
Metastasis	Normal to +++	−	Normal	− to −−−	+ to +++	Absent to +++
Acute infarct	+	−	++	− to −−	Absent	++ to ++++
Chronic infarct	Normal	−	−	Normal to −−	+++	+ to ++
Infection	Normal	Normal to −	+	− to −−	Absent	+
Multiple sclerosis (acute)	+	Normal	++	− to −−	Absent to ++	Absent to ++
Radiation necrosis	Absent to −−	Absent to −−	Absent to −−	Absent to −−	Absent to ++++	Absent to ++

Note.—Semiquantitative 9-point scale runs from −−−− to normal to ++++; − indicates decreased from normal, + indicates increased from normal. Lipid and lactate are normally absent.

is no difference in mean diagnostic performance among blinded readers for differentiating neoplasm from nonneoplasm (Table 1). The five statistics of diagnostic performance included sensitivity, specificity, PPV, NPV, and accuracy. The equivalence between the trapezoidal area (Aw) under an ROC curve and Wilcoxon's statistic can be used to test for statistically significant differences in Aw between pairs of ROC curves (16). However, our small, unbalanced sample size of 42 neoplastic and 13 nonneoplastic spectra, and a maximal pairwise difference in Aw of .10 (Table 2, reader A versus reader C) precluded such an analysis for a conventional level of statistical significance with type I error of .05, and type II error of .20 (16) (Table 2).

For each binary decision statistic (sensitivity, specificity, NPV, PPV, and accuracy), a paired two-tailed Student's t test (Instat) was used to test the null hypothesis that there is no difference in the mean value between untreated and treated patient subgroups among the small sample set of four blinded readers (Table 4). (The small sample size precluded the use of the nonparametric Mann-Whitney test.) For each comparison, statistical power (1 − type II error) was estimated under the convention that type I error be fixed at .05 (Stata). Similarly, for the fixed sample size of four readers and a conventional level of statistical significance with type I error of .05 and type II error of .20 (power = .80), the minimum detectable difference was

computed (Instat). This minimum statistically significant difference was also expressed as a percentage of the mean value for the whole patient group (average of readers A, B, C, and D; Table 1).

Results

Spectra from 55 brain lesions in 53 patients were included. (In two patients, two separate lesions were studied.) Histologic diagnoses were established for 50 lesions. Diagnoses were established in three cases of infarct by clinical follow-up and serial radiologic studies (CT, MR imaging, MR angiography, catheter angiography, or a combination) in which the lesions diminished in size. Diagnoses were established in two cases of acute demyelinating disease by clinical follow-up and reduction of lesion size on serial MR images. Examples of nonneoplastic cases in which the initial MR study suggested neoplasm are illustrated in Figures 1 and 2. The patients included 31 males and 22 females, with a mean age of 45 years (range, 14 to 81 years). Fourteen patients (15 lesions) had received
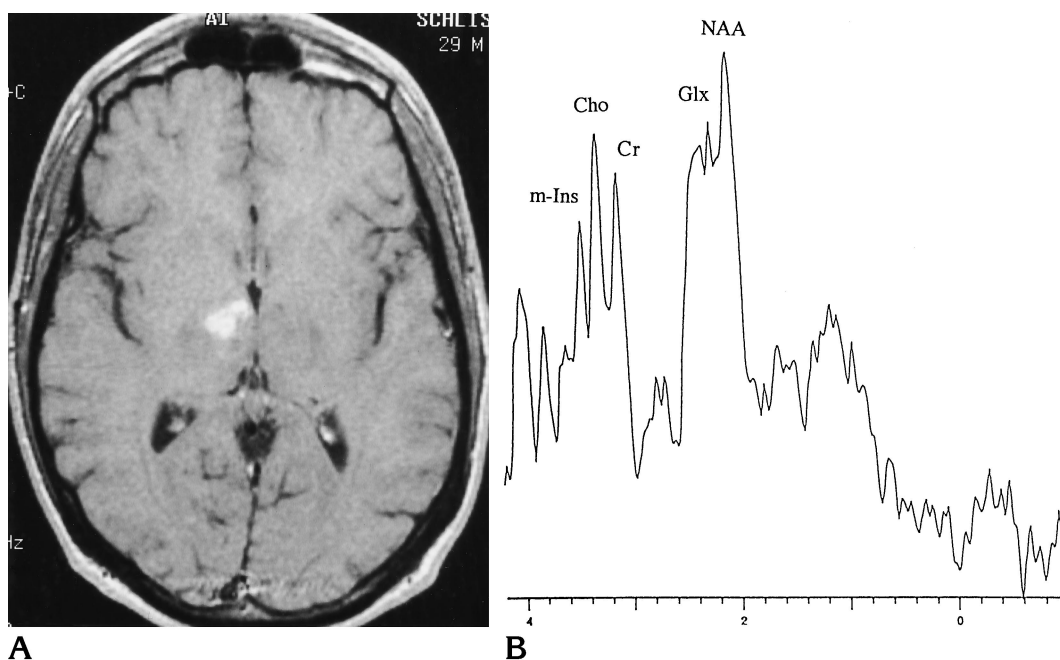
Fig 1. *A*, Axial contrast-enhanced T1-weighted MR image (600/20/2 [repetition time/echo time/excitations]) in a 29-year-old man shows an isolated, enhancing right thalamic lesion. No bright thalamic signal was noted on precontrast T1-weighted images (not shown).

B, Single-voxel proton spectrum (0.5 T, PRESS, echo time of 41) obtained from the lesion shows nonneoplastic features, including a mildly diminished NAA amplitude, no significant Cho elevation, and a broadening of the Glx peak with an increase in glutamate (2.35 ppm) relative to glutamine (2.45 ppm). A thalamic infarct was diagnosed at follow-up clinical examinations and by serial MR imaging studies, which showed a reduction in the lesion size, with cavitation.
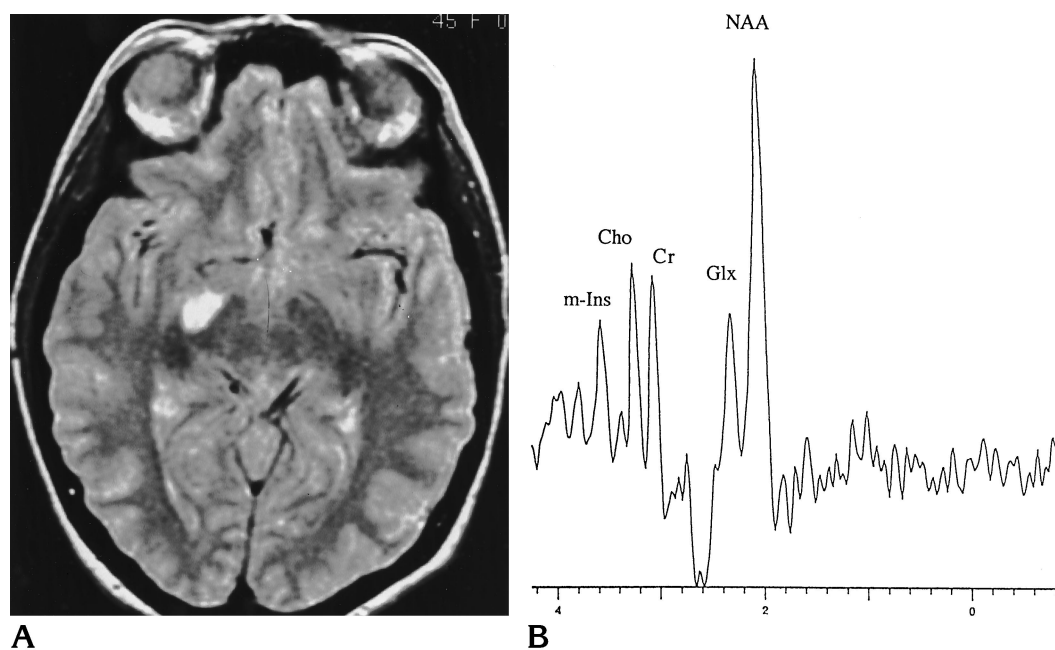

Fig 2. *A*, Axial proton density–weighted fast spin-echo image (3400/29 effective/1) in a 45-year-old woman shows an isolated lesion in the base of the right basal ganglia. Peripheral enhancement after contrast administration was seen on T1-weighted images (not shown).

B, Single-voxel proton spectrum (0.5 T, PRESS, echo time of 41) obtained from the lesion shows no reduction in the NAA resonance and no elevation in the Cho peak to suggest a neoplasm. Demyelinating disease was diagnosed at follow-up clinical examination and by serial MR imaging, which showed new lesions in the periventricular white matter and corpus callosum.

treatment for brain neoplasia before undergoing MR spectroscopy.

Distribution of the 42 final diagnoses of neoplasia was as follows: astrocytoma (not otherwise specified), one; astrocytoma grade IV (glioblastoma multiforme), 10; astrocytoma grade III, two; astrocytoma grade II, four; astrocytoma grade I, four; giant cell astrocytoma, one; oligodendroglioma, two; mixed glioma, four; ganglioglioma, one; ependymoma, one; meningioma, six; metastasis, four; dysembryoblastic neuroepithelial tumor, two. Distribution of the 13 nonneoplastic final diagnoses was as follows: Rathke's pouch cyst, one; infarct, three; parasitic infection, one; sarcoidosis, one; acute inflammation and gliosis, one; demyelinating disease, two; radiation necrosis without neoplasm, one; vasculitis, one; arteriovenous malformation with old hemorrhage and cavitated necrosis, one; neuroglial (gyral) dysplasia, one. Cases in which there was histologic evidence of posttreatment (surgery, radiation, chemotherapy, or a combination) effects and neoplasm were classified as neoplastic disease.

Spectra from all 10 control subjects were considered of diagnostic quality by all four blinded readers. Blinded readers disqualified 20 (9%) of 213 patient spectra as nondiagnostic because of unacceptably low SNRs, ambiguous resonance assignments, unacceptably broad resonances, lack of detectable metabolite resonances, equivocal findings of neoplasm versus nonneoplasm, or a combination of the above. Clerical errors in preparing spectra for blinded interpretations resulted in from one to three disqualified cases for each reader, for a total of seven cases.

Normal versus Abnormal Spectra

The sensitivity, specificity, PPV, NPV, and accuracy in differentiating normal from abnormal spectra for the four blinded readers averaged .97, .93, .99, .87, and .96, respectively (Table 1). The continuous (Az) and trapezoidal (Aw) areas under the aggregate ROC curve were both .99 (Table 2). ROC curves were not obtained for readers B, C, and D because the data were mathematically degenerate and implied near-perfect decision performance. Nonweighted κ statistics for interobserver agreement ranged from .76 (good) to .94 (very good) (13) (Table 3). The three false-positive errors were for spectra from healthy control subjects interpreted as
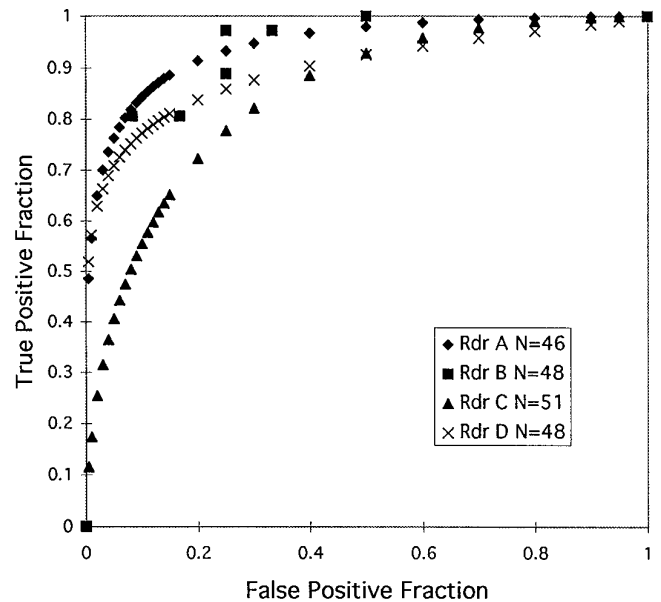

Fig 3. ROC curves for four blinded readers in the differentiation of neoplastic from nonneoplastic brain disease by single-voxel MR spectroscopy. Discrete ROC operating points are presented for reader B, since the algorithm to estimate a continuous ROC curve did not converge after 100 iterations.

abnormal but nonneoplastic. The five false-negative errors were for spectra from patients with sarcoidosis, gyral dysplasia, and acute demyelinating disease interpreted as normal.

Neoplastic versus Nonneoplastic Spectra

The sensitivity, specificity, PPV, NPV, and accuracy for neoplastic versus nonneoplastic spectra for the four blinded readers averaged .85, .74, .92, .61, and .83, respectively (Table 1). ROC curves for the blinded readers are presented in Figure 3. The continuous (Az) and trapezoidal (Aw) areas under the aggregate ROC curve were .84 and .89, respectively (Table 2). Readers A and B had slightly greater accuracy than readers C and D, commensurate with more experience with clinical MR spectroscopy. However, a P value of .15 (ANOVA) revealed no statistically significant difference in diagnostic performance among the blinded readers. Similarly, the trapezoidal areas (Aw) under the ROC curves for readers A and B slightly exceeded those of readers C and D. However, Wilcoxon's test to determine any statistically significant differences in Aw between pairs of readers was beyond the scope of the current study. Nonweighted κ statistics for in-

terobserver agreement ranged from .51 (moderate) to .64 (good) (13) (Table 3).

In general, the sensitivity, specificity, PPV, NPV, and accuracy of MR spectroscopy for the untreated patients exceeded those for the treated patients for each blinded reader (Table 4). P values from Student's t test comparing the mean values of sensitivity, specificity, PPV, NPV, and accuracy for neoplasm versus non-neoplasm in the treated versus untreated patient subgroups were .21, .06, .60, .01, and .06, respectively. For a fixed type I error of .05 and a sample size of four blinded readers, the corresponding estimated powers (1 − type II error) for sensitivity, specificity, and so on were 0.25, 0.56, 0.05, 1.00, and 0.63, respectively. The corresponding minimum differences detectable with statistical significance under conventional levels of type I error of .05, type II error of .20 (power = .80) and four samples were .21 (25% of the average sensitivity of readers A, B, C, and D for all patients in Table 1), .33 (45% of the average specificity of readers A, B, C, and D), .12 (13% of the average PPV of readers A, B, C, and D), .41 (67% of the average NPV of readers A, B, C, and D), and .97 (12% of the average accuracy of readers A, B, C, and D), respectively.

Nonblinded readers generated 40 true-positive, 12 true-negative, no false-positive, and two false-negative results. One spectrum of the 55 brain lesions in the study (1.8%) was interpreted as nondiagnostic (equivocal) in the discrimination of neoplasm from nonneoplasm. The sensitivity, specificity, PPV, NPV, and accuracy for the nonblinded readers was 0.95, 1.00, 1.00, 0.86, and 0.96, respectively (Table 1).

Among the blinded readers, 12 false-positive errors (nonneoplastic lesions interpreted as neoplastic) were made in eight brain lesions, two of which had been treated. The spectra were dominated by mobile lipids in eight of the errors. These eight lesions included an ischemic infarction, radiation necrosis following treatment of a metastasis, vasculitis with infarction, a treated cerebral arteriovenous malformation with cavitated necrosis and hemorrhage, gliosis in the left cerebellar peduncle, craniopharyngioma, demyelinating disease, and cerebellar infarction.

Among the blinded readers, 22 false-negative errors (neoplastic lesions interpreted as non-neoplastic) were made in 13 lesions, four of which had been treated. The amplitudes of the mobile lipid resonances were comparable to or greater than NAA in 12 of the 22 errors. These 13 lesions included glioblastoma, treated glioblastoma, astrocytoma grade I, astrocytoma grade II, treated astrocytoma grade III-IV, oligodendroglioma, treated metastasis, and meningioma.

Discussion

Clinical MR spectroscopy at 0.5 T is feasible (11) (Prost et al, "0.5 T H-1 Spectroscopy..."). It demonstrates elevated Cho and decreased NAA resonance amplitudes in primary and secondary brain neoplasms. Since the chemical shift (ppm) is independent of field strength, resonance assignments of uncoupled spins are identical at 0.5 T and 1.5 T, and assignments of weakly J-coupled spins are similar at the two field strengths. The absolute spectral dispersion (units of Hz) is reduced by a factor of 3.0 while the SNR of the NAA singlet resonance is reduced by a factor of 1.4 in operating at 0.5 T relative to 1.5 T, with otherwise identical systems (11). However, advantages of 0.5 T over 1.5 T for MR spectroscopy include reduced spectral distortion from local magnetic field susceptibility changes due to blood, calcium, or interfaces between brain and bone; reduced repetition times for comparable degrees of longitudinal relaxation between repeated excitations (thus shorter examinations); and increased SNR of the combination (Glx) of glutamine and glutamate brain resonances by a factor of two. The dissemination of MR spectroscopic techniques at 0.5 T would increase the availability of proton spectroscopy (17).

While several investigators have studied the role of MR spectroscopy in the prediction of tumor grade (1, 7), a study of the accuracy of MR spectroscopy in the differentiation of normal from abnormal brain tissue and neoplasm from nonneoplasm based on blinded interpretations by visual inspection has not to our knowledge been reported. Preul et al accurately distinguished all 91 patients with known brain neoplasms from 14 control subjects using a statistical linear discriminant analysis applied to the ratio of brain metabolites to the contralateral Cr amplitude (M. C. Preul, Z. Caramanos, D. L. Collins, J-G. Villemure, W. Feindel, D. L. Arnold, "Linear Discriminant Analysis Based on Proton MR Spectroscopic Imaging of Human

Brain Tumours Improves Pre-Operative Diagnosis," presented at the annual meeting of the Society of Magnetic Resonance in Medicine, San Francisco, Calif, August 1994). Unlike Preul et al, we included patients with nonneoplastic brain diseases and patients who had received prior cancer treatment.

The diagnostic accuracy in our series of nonblinded MR spectroscopy interpretations of neoplasm versus nonneoplasm (.96) was comparable to that reported by Sorby (18) for MR imaging in brain neoplasms (.93). A direct comparison of our results to Sorby's is difficult because Sorby's series of 431 neoplasms included 42 (10%) tumorlike conditions (ie, petrous apex cholesterol cyst) and 138 (32%) midline pineal and pituitary lesions, which were not represented in our patient group. Furthermore, Sorby's report does not state whether any patients had received prior treatment for brain neoplasms. Our sensitivity in the blinded MR spectroscopic discrimination of neoplasm from nonneoplasm (.85) was the same as that with 1.5-T MR imaging in one series for the neoplastic disease category (.85) (19) and midway between that of benign (.74) and malignant (.94) neoplasms with MR imaging at 0.5 T to 1.5 T in another series (20). Our nonblinded MR spectroscopic sensitivity (.95) exceeded that in both studies. The diagnostic accuracy and specificity statistics were not explicitly stated in the other series. A comparison of the diagnostic accuracy with blinded MR spectroscopy versus MR imaging (without MR spectroscopy) was beyond the scope of the current study.

The three false-positive findings in our study in the discrimination of normal from abnormal spectra were not interpreted as neoplastic disease. MR spectroscopy obtained from normal brain structures with equivocal or artifactual signal changes on MR images are therefore unlikely to be interpreted as neoplastic. Conversely, none of the five false-negative interpretations were made in patients with neoplasms. MR spectra obtained from neoplastic tissue are unlikely to be interpreted as normal.

Errors in discriminating neoplastic from nonneoplastic disease were made in lipid-rich spectra. Twelve of 22 false-negative interpretations were made in cases with large lipid resonances. With our techniques, lipid signal is more likely to be due to cellular necrosis than to contamination by scalp fat. Sampling necrotic portions of the tumor with a paucity of active membrane

degradation or synthesis is therefore likely to cause false-negative errors (8–10). In our experience, false-negative interpretations of spectra with abundant lipid resonances tended to occur in cases of higher grade gliomas and metastases. Eight of 12 false-positive errors were made in lipid-rich spectra. In three of these lesions, metabolites other than lipid were poorly resolved, as the dynamic range of the detector was dominated by lipid. Therefore, when single-voxel MR spectroscopy reveals large lipid peaks, the accuracy of discriminating neoplasm from nonneoplasm is reduced. An additional spectrum from a different location in the lesion may be useful.

Diminished NAA and markedly elevated Cho resonances have been reported in several non-neoplastic conditions, including in healthy neonates (21, 22), in cases of X-linked adrenoleukodystrophy (23), in patients who have sustained trauma (24), in patients who have had liver transplantation (24), in the subacute (recovery) phase of global hypoxic-ischemic injury (25), in cases of progressive multifocal leukoencephalopathy in patients with acquired immunodeficiency syndrome (26), and in animals in the acute inflammatory phase of experimental allergic encephalomyelitis that precedes demyelination (27). A modest reduction in NAA and a mild elevation of Cho have been reported in acute (28) (P. Christiansen, H. B. W. Larsson, O. Henriksen, "Time Dependence of N-Acetylaspartate an Choline Containing Compounds in Multiple Sclerosis," presented at the annual meeting of the Society of Magnetic Resonance in Medicine, August 1993; and C. A. Davie, C. P. Hawkins, G. J. Barker, et al, "Serial Proton MRS in Demyelination," presented at the annual meeting of the Society of Magnetic Resonance in Medicine, August 1993), and chronic (29) multiple sclerosis, with a maximal elevation of Cho in the subacute period. A decrease in NAA intensity by as much as 70% relative to contralateral brain and an increase in Cho by as much as 180% have been observed in a small series of four patients with single large demyelinating lesions (N. De Stefano, M. Preul, P. M. Matthews, G. S. Francis, J. P. Antel, D. L. Arnold, "Metabolic Changes in Acute Demyelinating Plaques Studied Longitudinally by Proton MR Spectroscopic Imaging," presented at the annual meeting of the Society of Magnetic Resonance in Medicine, San Francisco, Calif, August 1994). The descriptions of these four le-

sions resembled those in a recent series of demyelinating lesions that mimicked neoplasms on imaging studies (30). As these conditions and diseases were not represented in our series, their influence on the accuracy of MR spectroscopy in the discrimination of neoplasm from nonneoplasm warrants further study.

A limitation of the current study is that the biopsy specimen in patients who underwent a procedure may not have included the portion of the lesion sampled with MR spectroscopy, since the biopsy was done at the discretion of the surgeon. Sampling errors in MR spectroscopy may be improved with the use of two-dimensional chemical-shift imaging, in which a grid of voxels is placed over a lesion and a spectrum is generated from each element in the grid, at the cost of increasing the examination time. In the future, this technique might assist the surgeon in obtaining tissue from the most metabolically active portion of a lesion, and perhaps influence the choice between an open or a closed stereotactic procedure (31).

Conclusions

Proton spectra obtained at 0.5 T with the image-guided single-voxel technique accurately differentiate healthy control subjects from patients with suspected brain neoplasms on CT or MR imaging studies. Clinical MR spectroscopy in patients with suspected neoplasms or recurrent neoplasia can differentiate neoplastic from nonneoplastic disease with a high diagnostic accuracy. MR spectroscopy together with MR imaging achieves a higher diagnostic accuracy than MR spectroscopy alone. Readers are prone to both false-positive and false-negative errors in interpreting spectra with large mobile lipid resonances in the 0.5-to-1.5-ppm range.

Acknowledgments

References

1. Negendank WG, Sauter R, Brown TR, et al. Proton magnetic resonance spectroscopy in patients with glial tumors: a multicenter study. *J Neurosurg* 1996;84:449–458

2. Yamagata NT, Miller BL, McBride D, et al. In vivo proton spectroscopy of intracranial infections and neoplasms. *J Neuroimaging* 1994;4:23–28

3. Demaerel P, Johannik K, Van Hecke P, et al. Localized H-1 NMR spectroscopy in fifty cases of newly diagnosed intracranial tumors. *J Comput Assist Tomogr* 1991;15:67–76

4. Miller BL, McBride D, Riedy G, Caron M, Lipcamon J, O'Brien D. Changes in brain choline in tumors with H-1 NMR spectroscopy. *Bull Clin Neurosci* 1990;55:115–122

5. Sijens PE, Knopp MV, Brunetti A, et al. H-1 MR spectroscopy in patients with metastatic brain tumors: a multicenter study. *Magn Reson Med* 1995;33:818–826

6. Bruhn H, Frahm J, Gyngell ML, et al. Noninvasive differentiation of tumors with use of localized H-1 MR spectroscopy in vivo: initial experience in patients with cerebral tumors. *Radiology* 1989;172: 541–548

7. Poptani H, Gupta RK, Roy R, Pandey R, Jain VK, Chhabra DK. Characterization of intracranial mass lesions with in vivo proton MR spectroscopy. *AJNR Am J Neuroradiol* 1995;16:1593–1603

8. Segebarth CM, Baleriaux DF, Luyten PR, den Hollander JA. Detection of metabolic heterogeneity of human intracranial tumors in vivo by H-1 NMR spectroscopic imaging. *Magn Reson Med* 1990; 13:62–76

9. Ott D, Hennig J, Ernst T. Human brain tumors: assessment with in vivo proton MR spectroscopy. *Radiology* 1993;186:745–752

10. Fulham MJ, Bizzi A, Dietz MJ, et al. Mapping of brain tumor metabolites with proton MR spectroscopic imaging: clinical relevance. *Radiology* 1992;185:675–686

11. Prost RW, Mark L, Mewissen M, Li S. Detection of glutamate/glutamine resonances by H-1 magnetic resonance spectroscopy at 0.5 tesla. *Magn Reson Med* 1997;37:615–618

12. Dawson-Saunders B, Trapp RG. *Basic & Clinical Biostatistics.* 2nd ed. Norwalk, Conn: Appleton & Lange; 1994:213

13. Fisher LD, van Belle G. *Biostatistics: A Method for the Health Sciences.* New York, NY: Wiley; 1993:206–209, 256–259

14. McNeil BJ, Keeler E, Adelstein SJ. Primer on certain elements of medical decision making. *N Engl J Med* 1975;293:211–215

15. Swets JA, Pickett RM, Whitehead SF, et al. Assessment of diagnostic technologies. *Science* 1979;205:753–759

16. Hanley JA, McNeil BJ. The meaning and use of the area under a receiver operating characteristic (ROC) curve. *Radiology* 1982; 143:29–36

17. Cousins JP. Clinical MR spectroscopy: fundamentals, current applications, and future potential. *AJR Am J Roentgenol* 1995;164: 1337–1347

18. Sorby WA. An evaluation of magnetic resonance imaging at the Royal North Shore Hospital of Sydney, 1986–1987. *Med J Aust* 1989;151:8–18

19. Orrison WW, Stimac GK, Stevens EA, et al. Comparison of CT, low-field-strength MR imaging, and high-field-strength MR imaging: work in progress. *Radiology* 1991;181:121–127

20. Haughton VM, Rimm AA, Sobocinski KA, et al. A blinded clinical comparison of MR imaging and CT in neuroradiology. *Radiology* 1986;160:751–755

21. Kreis R, Ernst T, Ross BD. Development of the human brain: in vivo quantification of metabolite and water content with proton magnetic resonance spectroscopy. *Magn Reson Med* 1993;30: 424–437

22. Toft P, Leth H, Lou HC, Pryds O, Henriksen O. Metabolite concentrations in the developing brain estimated with proton MR spectroscopy. *J Magn Reson Imaging* 1994;4:674–680

23. Kruse BK, Barker PB, van Zijl PCM, Duyn JH, Moonen CTW,

Moser HW. Multislice proton magnetic resonance spectroscopic imaging in X-linked adrenoleukodystrophy. *Ann Neurol* 1994;36: 595–608

24. Ross BD, Moats R, Michaelis T, Mandingo JC. Neurospectroscopy. In: *Introductory and Advanced MRI: Techniques and Clinical Applications.* Berkeley, Calif: Society of Magnetic Resonance; 1994:120–126

25. Ross BD, Lee JH, Moats RA. Clinical MRS for clinical radiologists. In: *Clinical MR Refresher Course.* Berkeley, Calif: Society of Magnetic Resonance; 1993:109–115

26. Chiang L, Miller BL, McBride D, et al. Brain lesions in patients with AIDS: H-1 MR spectroscopy. *Radiology* 1995;197:525–531

27. Brenner RE, Munro PMG, Williams SCR, et al. The proton NMR spectrum in acute EAE: the significance of the change in the cho:cr ratio. *Magn Reson Med* 1993;29:737–745

28. Roser W, Hagberg G, Mader I, et al. Proton MRS of gadolinium-enhancing MS plaques and metabolic changes in normal-appearing white matter. *Magn Reson Med* 1995;33:811–817

29. Arnold DL, Matthews PM, Francis G, Antel J. Proton magnetic resonance spectroscopy of human brain in vivo in the evaluation of multiple sclerosis: assessment of the load of the disease. *Magn Reson Med* 1990;14:154–159

30. Kepes JJ. Large focal tumor-like demyelinating lesions of the brain: intermediate entity between multiple sclerosis and acute disseminated encephalomyelitis? A study of 31 patients. *Ann Neurol* 1993;33:18–27

31. Franzini A, Leocata F, Giorgi C, Allegranza A, Servello D, Broggi G. Role of stereotactic biopsy in multifocal brain lesions: considerations in 100 consecutive cases. *J Neurol Neurosurg Psychiatry* 1994;57:957–960